

1

2 **Supplementary Information for**

3 **Strong spatial embedding of social networks generates non-standard epidemic dynamics** 4 **independent of degree distribution and clustering**

5 **David J. Haw, Rachael Pung, Jonathan M. Read, Steven Riley**

6 **Corresponding Author: Steven Riley.**

7 **E-mail: s.riley@imperial.ac.uk**

8 **This PDF file includes:**

9 Supplementary text

10 Figs. S1 to S12

11 Tables S1 to S2

12 References for SI reference citations

13 **Supporting Information Text**

14 **Protocol S1: analytic approximations**

Derivation of degree distribution and global clustering coefficient.

$$\begin{aligned}
\langle k \rangle &= h - 1 + (w - 1 - \langle \text{housemates at workplace} \rangle) p_w \\
&\approx h - 1 + p_w (w - 1) \\
P(K = k) &= \sum_{1 \leq i \leq k+1} P(H = i) \sum_{j-1 \geq k-i+1} P(W = j) \\
&\times \binom{j-1}{k-i+1} p_w^{k-i+1} (1-p_w)^{j-1-k+(i-1)} \\
&= \sum_{1 \leq i \leq k+1} \frac{(h-1)^{i-1} e^{1-h}}{(i-1)!} \sum_{j \geq k-i+2} \frac{(w-1)^{j-1} e^{1-w}}{(j-1)!} \\
&\times \binom{j-1}{k-i+1} p_w^{k-i+1} (1-p_w)^{j-k+i-2} \\
\langle CC^1 \rangle &\approx \frac{(h-1)(h-2) + p_w [p_w(w-1) - 1] [p_w(w-1) - 2]}{\langle k \rangle (\langle k \rangle - 1)}
\end{aligned}$$

15 where denominator = $\frac{1}{2}E(\text{potential contacts between neighbours})$ and numerator $\approx \frac{1}{2}E(\text{actual contacts between neighbours})$.

16 **Metapopulation approximation.** We now consider a metapopulation approximation to our network model, within the framework
17 of renewal equations. This will allow us to use existing theory in order to interpret our results.

18 Let i, j, k index the households in a given population, h the mean household size and $\langle k \rangle$ the mean contact rate of an individual
19 (this notation is consistent with mean degree the corresponding network model). We let K_{ij} denote the connection density between
20 households such that $K_{ii} = 0 \forall i$ and $\sum_j K_{ij} = 1 \forall j$, and we define the workplace contact rate $v = \langle k \rangle - h + 1 = p_w(w - 1)$.

21 The expected force of infection on an individual in household i (denoted $\langle \lambda_{[i]} \rangle$) is then given by:

$$\langle \lambda_{[i]} \rangle = \frac{\beta}{\langle k \rangle} \left[I_i + \frac{v}{h} \sum_j K_{ij} I_j \right] \quad [1]$$

22 where the denominator h comes from the fact that $\sum_j K_{ij} \langle N_j \rangle = h$, where $\langle N_j \rangle = h$ denotes the expected population of
23 household j .

The parameter $\hat{\rho} := h/v$ controls the diagonal weighting of the global coupling kernel $E + \hat{\rho}K$, where E denotes the $n \times n$
identity matrix (avoiding confusion with I , which is reserved for infectious populations). Furthermore, our spatial coupling
parameter α appears explicitly in K :

$$K_{ij} \propto \frac{1}{1 + (d_{ij}/a)^\alpha} \quad [2]$$

24 Note that, though K is typically called a "travel kernel", we are describing a static network structure with no (explicit) travel.
25 Also, the household/workplace framework does not lend itself to a description in continuous space, since households correspond
26 to single points in which finitely many agents are densely connected. We can, however, proceed with one continuous variable
27 per household and, for any given population density, we can define a discrete space in which each location contains (at most)
28 one household.

29 The presence of local decay in infectives *whilst the global epidemic is still growing* also renders the system described in
30 Equation Eq. (1) somewhat intractable analytically. However, if we view the force of infection $\langle \lambda_{[i]} \rangle$ as follows:

$$\langle \lambda_{[i]} \rangle = \langle \lambda_{[i]}^{in} \rangle + \langle \lambda_{[i]}^{out} \rangle \quad [3]$$

$$= \frac{\beta}{\langle k \rangle} I_i + \frac{\beta}{\hat{\rho} \langle k \rangle} \sum_j K_{ij} I_j \quad [4]$$

31 then the limiting cases $v \rightarrow 0$ and $h \rightarrow 1$ provide additional insight into the different growth phases observed. The first growth
32 phase is simply the mass-action SIR model, and the final, accelerating wave-like phase is related to the continuous-space model
33 defined by:

$$\lambda(t; \mathbf{x}) = \tilde{\beta} \frac{\int I(t; \mathbf{y}) K(\mathbf{x} - \mathbf{y}) d\mathbf{y}}{\int N(\mathbf{z}) K(\mathbf{x} - \mathbf{z}) d\mathbf{z}} \quad [5]$$

34 Moreover, both of these limiting cases are covered substantially in the literature. In particular, we draw the reader's attention
35 to the continuous space case, in which radial wave solutions are known to exist for $\alpha > 3$, with constant speed for $\alpha > 4$ and
36 accelerating for $\alpha \in (3, 4]$ (1–4).

37 **Codes**

38 All data generated and analysed in this study are provided in the GitHub repository www.github.com/c97sr/id_spatial_sim.

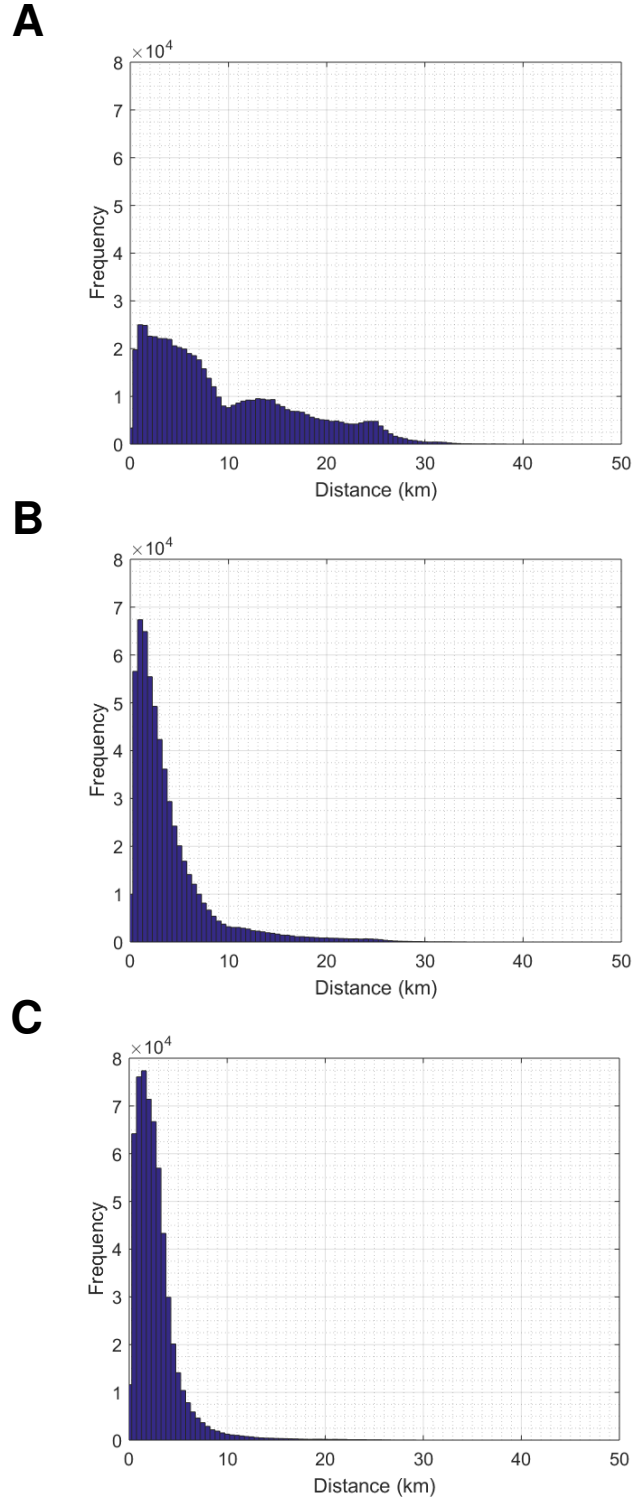


Fig. S1. Examples of commuting distributions for (A) $\alpha = 0$, (B) $\alpha = 3$ and (C) $\alpha = 6$. All networks use population of Monrovia, with $h = 4$, $w = 50$ and $p_w = 0.14$, so $\langle k \rangle = 10$.

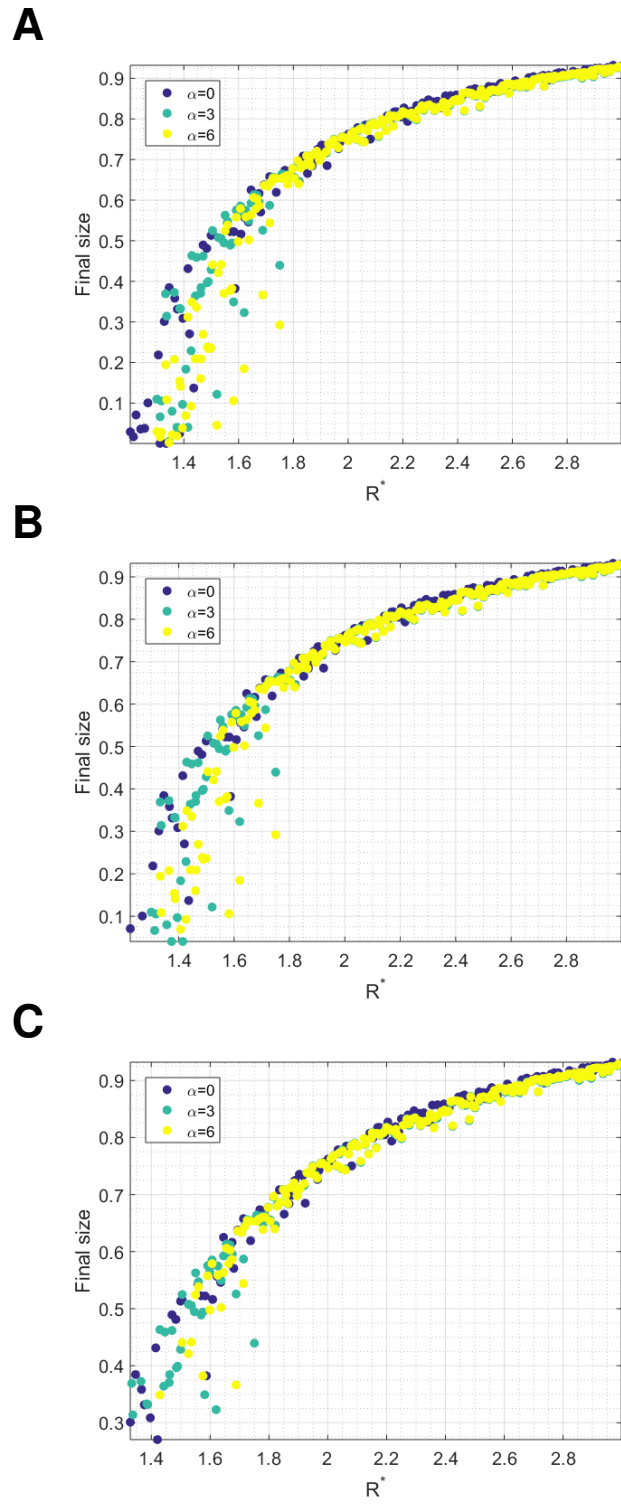


Fig. S2. The relationship between R^* and final size for (A) all simulations (B) all with peak over 100 and (C) peak over 500 (all simulations have seed size 10).

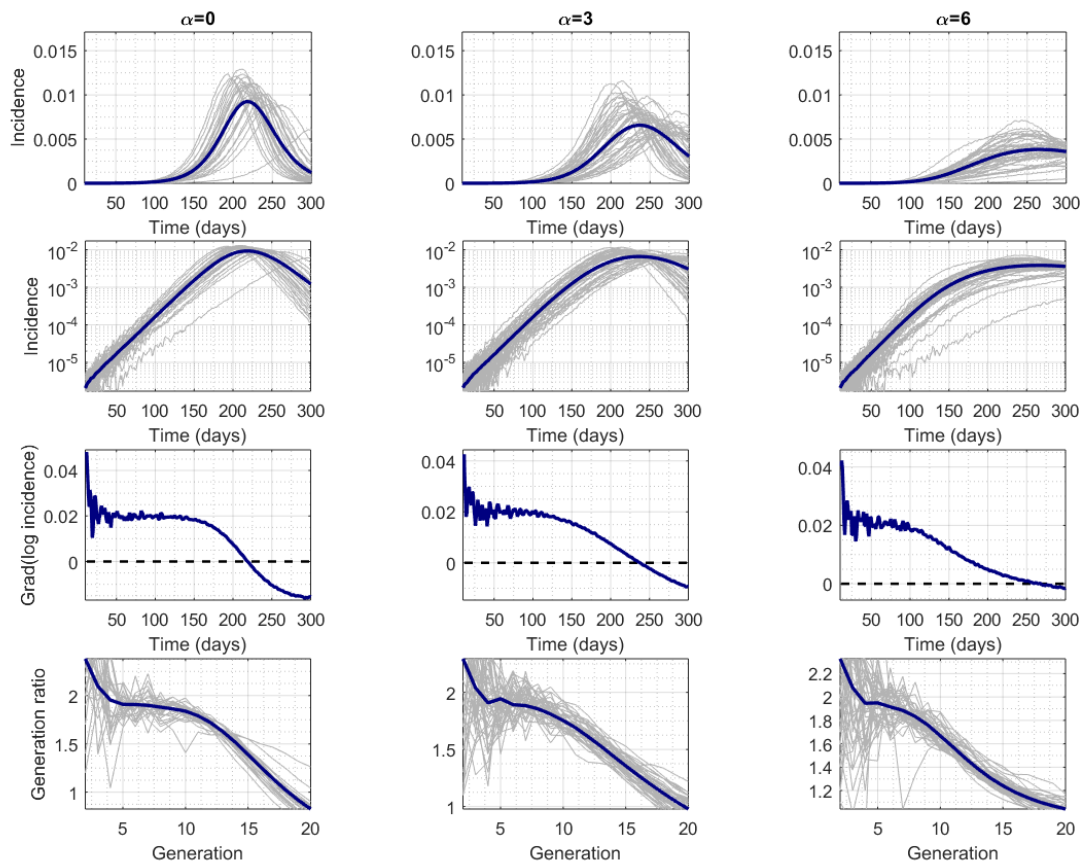


Fig. S3. Simulation results for $R_0 \in [1.8, 2)$, $\alpha = 0, 3, 6$.

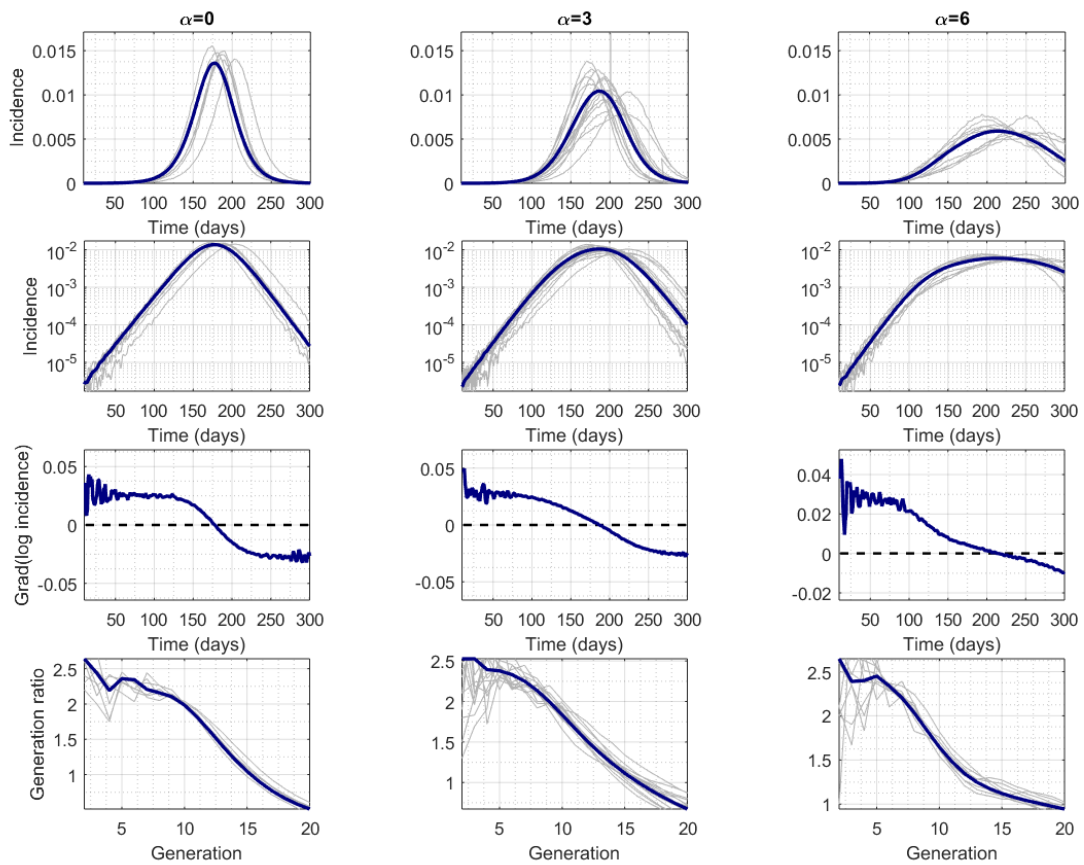


Fig. S4. Simulation results for $R_0 \in [2.2, 2.4)$, $\alpha = 0, 3, 6$.

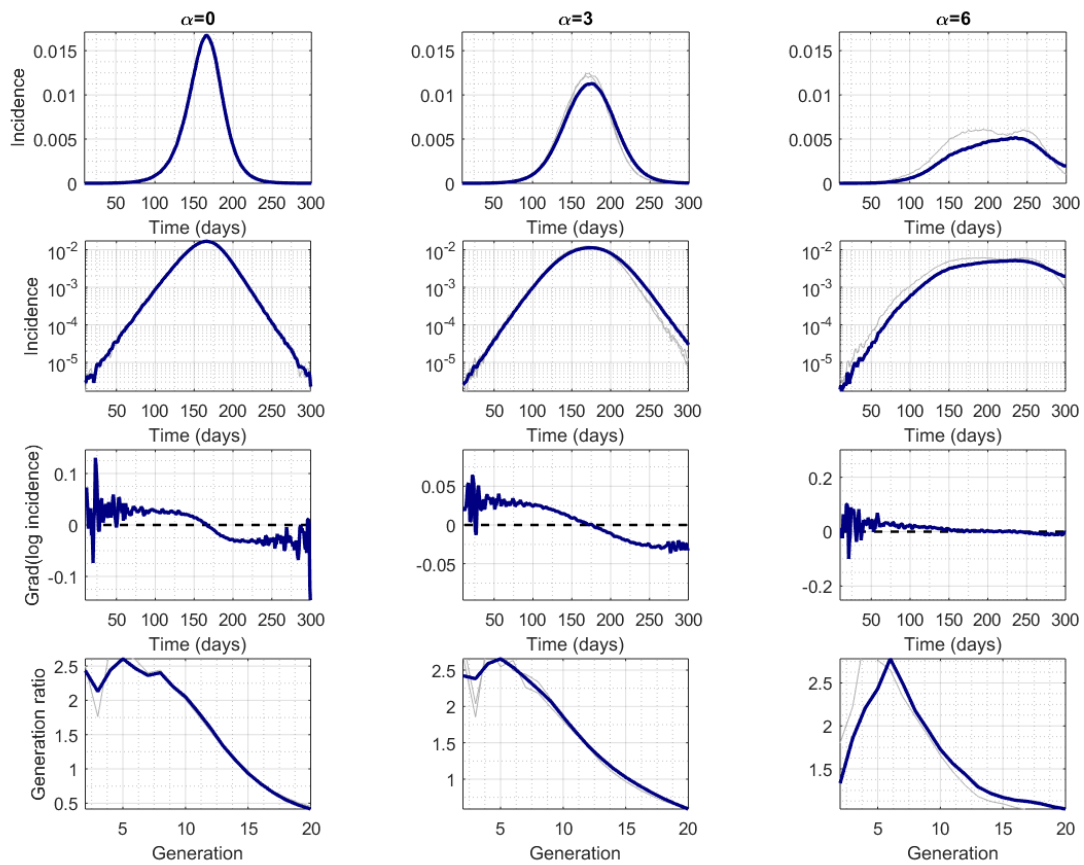


Fig. S5. Simulation results for $R_0 \in [2.4, 2.6)$, $\alpha = 0, 3, 6$.

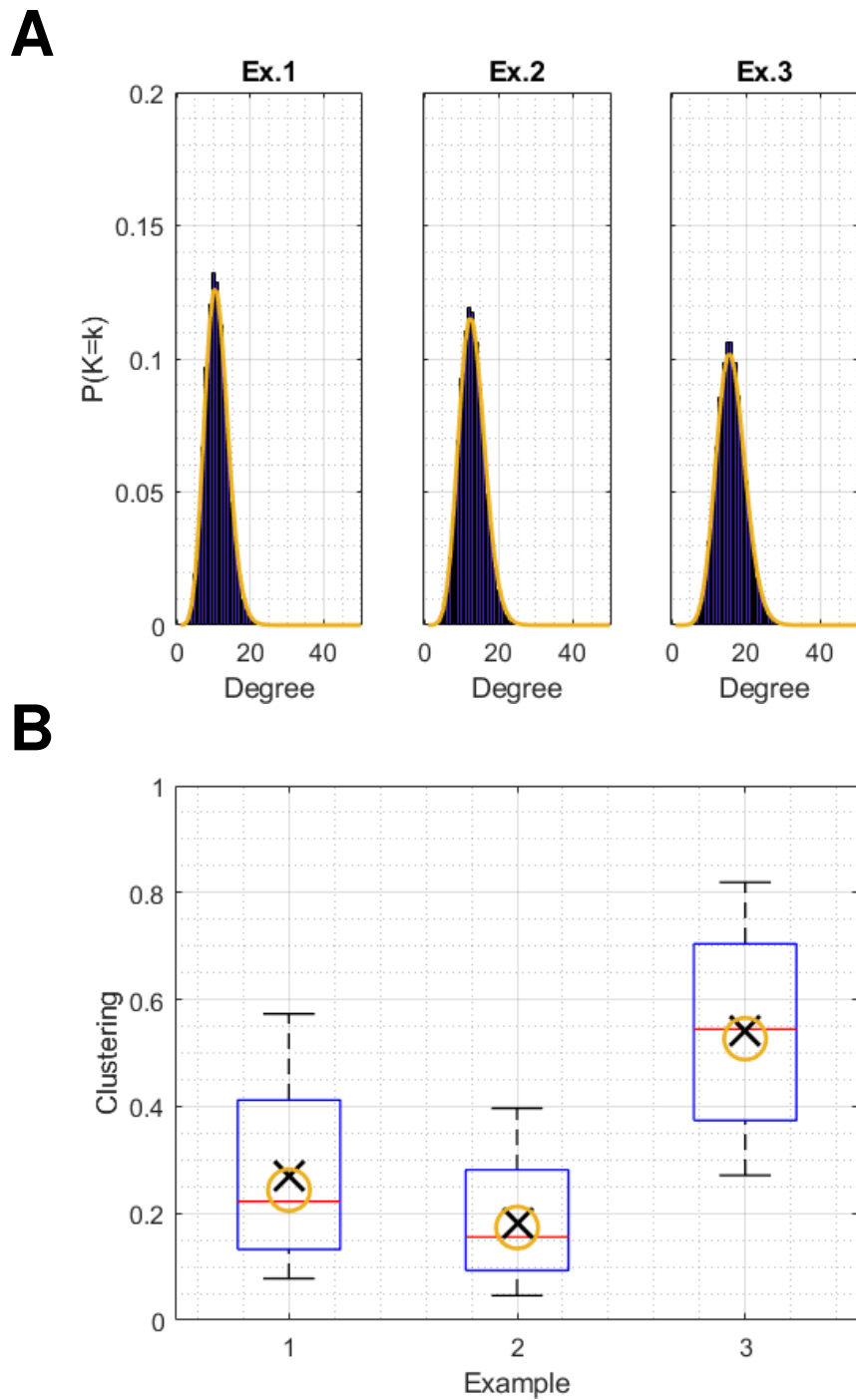


Fig. S6. (A) Degree distribution, and (B) clustering coefficient for 3 example networks, with analytic approximations for $P(K = k)$ and $\langle CC^1 \rangle$ shown in yellow. Example 1: $h = 6, w = 50, p_w = 0.1, v = 5, \langle k \rangle = 10$; example 2: $h = 6, w = 100, p_w = 0.07, v = 5, \langle k \rangle = 10$; example 3: $h = 11, w = 80, p_w = 0.05, v = 4, \langle k \rangle = 14$.

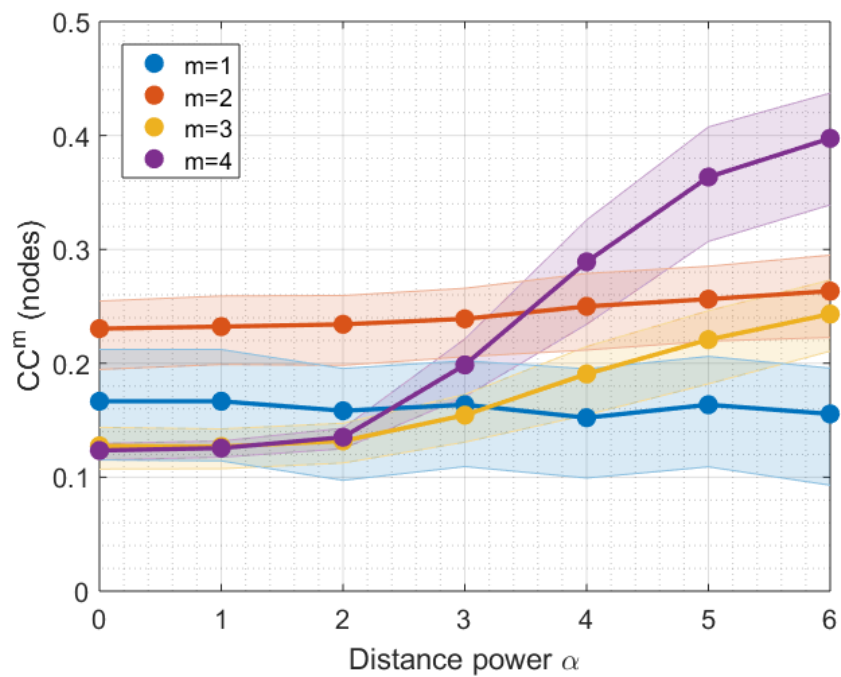


Fig. S7. Relationship between spatial correlation parameter α and clustering order 1 to 4 on a uniform population, defined as a 50×50 , 1km^2 grid with a population of 20 per pixel, and $h = 5$, $w = 50$, $p_w = 0.14$, $v = 7$, $\langle k \rangle = 11$ as in main Figure 4.

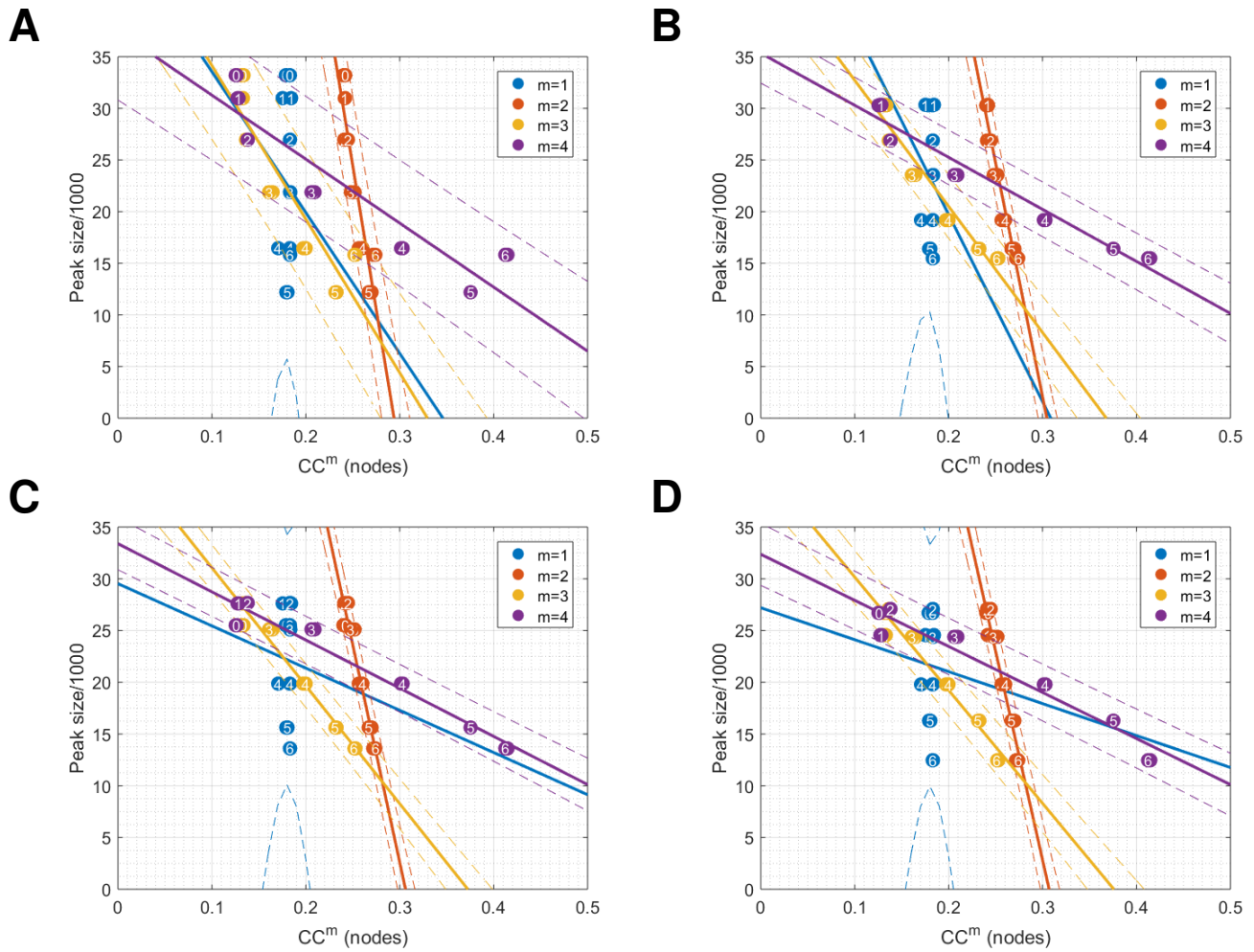


Fig. S8. Relationship between order- m clustering an epidemic peak height on the uniform population defined in Figure S7: (A) $R_0 \in [1.8, 2)$, (A) $R_0 \in [2, 2.2)$, (A) $R_0 \in [2.2, 2.4)$, (A) $R_0 \in [2.4, 2.6)$.

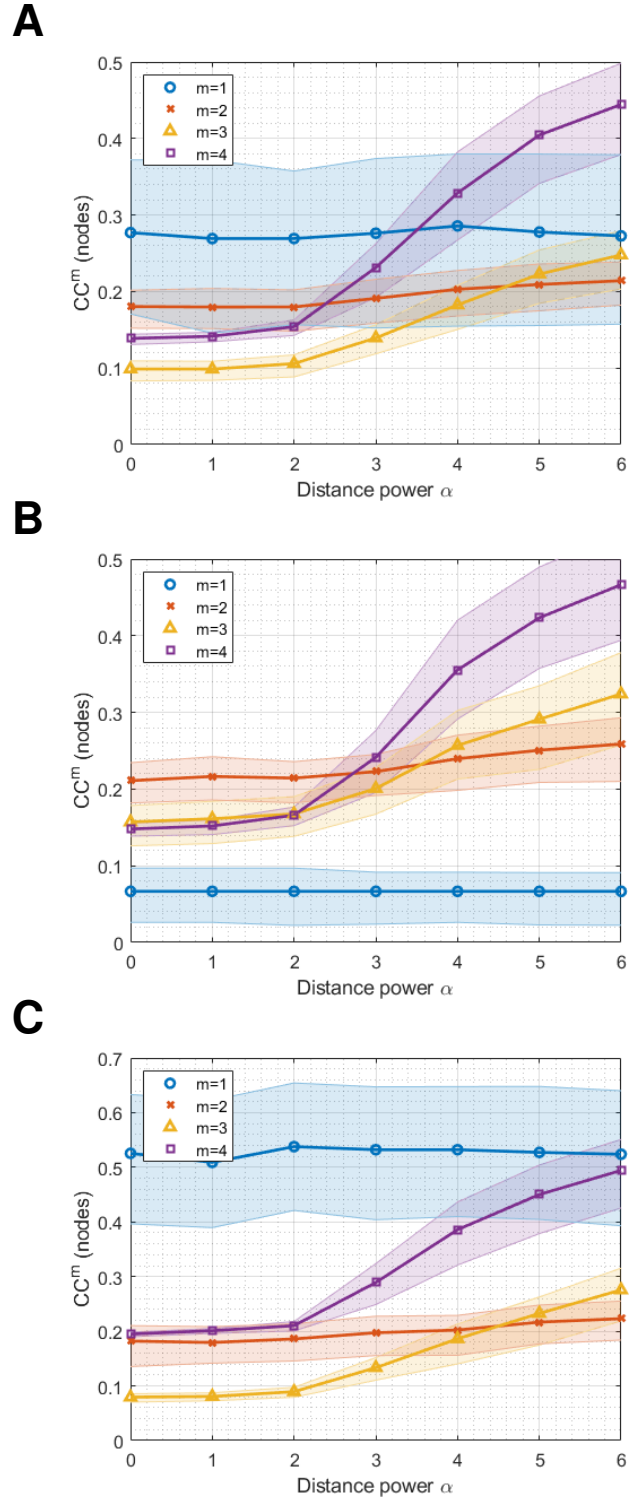


Fig. S9. Sensitivity analysis: clustering orders 1 TO 4 for $\alpha = 0, 1, \dots, 7$ for a sample of 1000 nodes on networks with (A) $h = 6, w = 100, p = 0.05$; (B) $h = 3, w = 200, p = 0.04$; (C) $h = 12, w = 100, p = 0.04$.

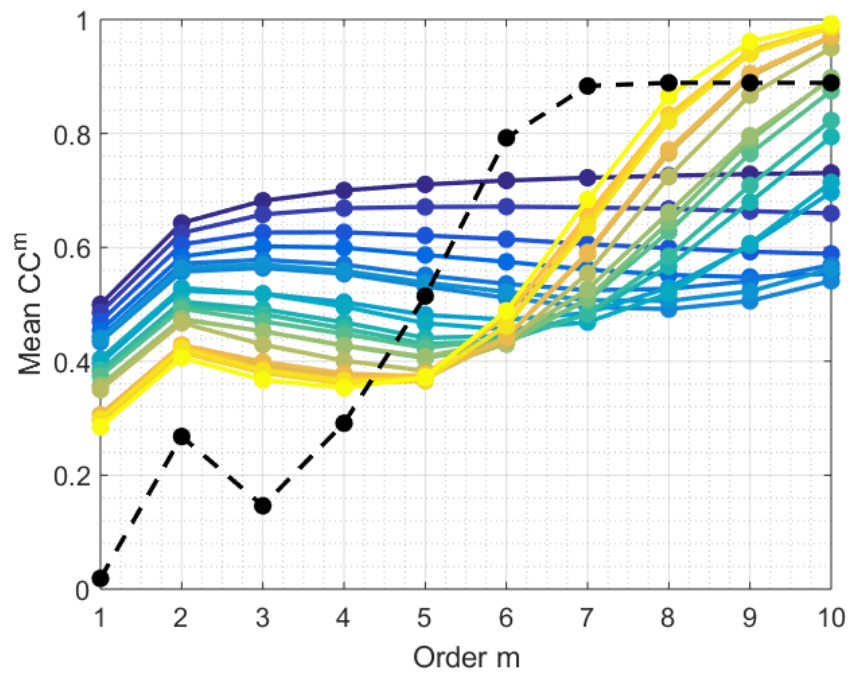
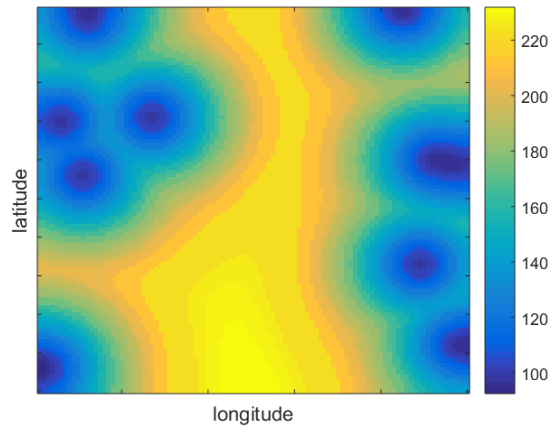


Fig. S10. Illustration of higher order clustering in Watts-Strogatz Small World networks $G(n, m, p)$. We fix number of nodes $n = 10^3$ and mean degree $k = 4$. Rewiring probability ranges from 0 (blue) to 0.2 (yellow). The black dotted line shows values for random graphs ($p = 1$).

A



B

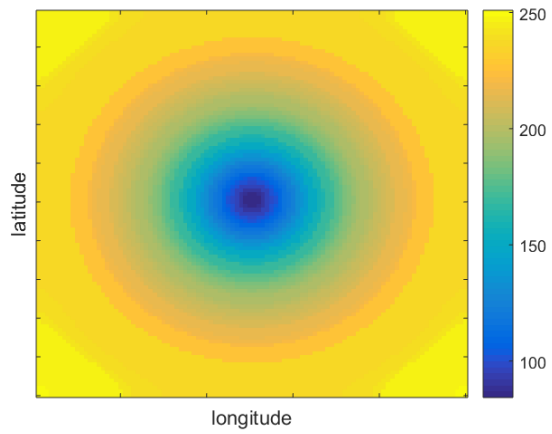


Fig. S11. Peak times for $\alpha = 6$: (A) seeding in 10 random locations and (B) seeding in the centre.

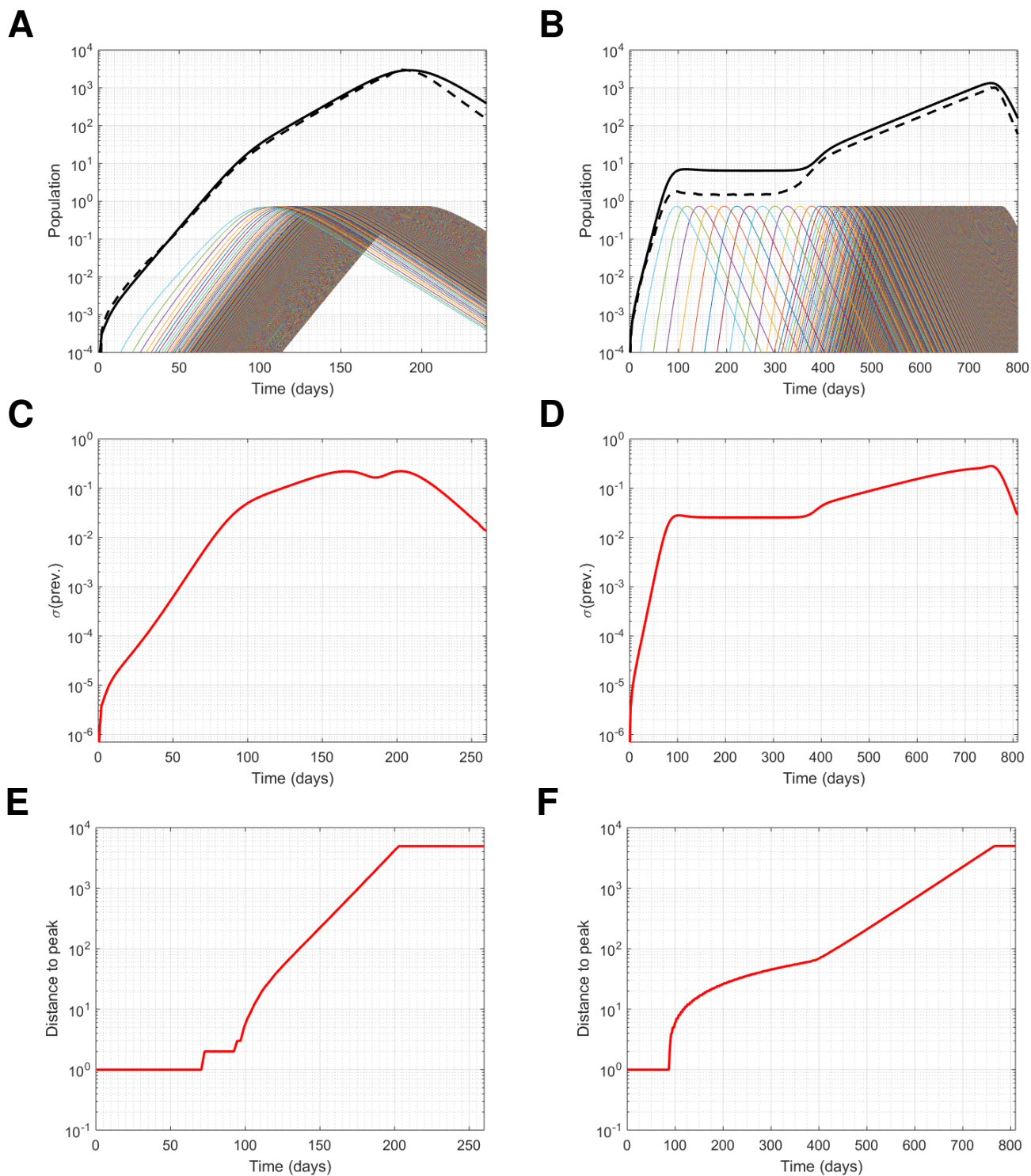


Fig. S12. Mean-field approximation with $\langle k \rangle = 10$, $h = 4$, using a 1×5000 grid (1D model) of uniformly spaced households and seeding at one end: (A) global prevalence (solid black line), global incidence (dashed line) and local prevalence in every 5th location (colored lines), (C), standard deviation of prevalence, (E) distance to peak prevalence for $\alpha = 2$, (B), (D), (F) the same with $\alpha = 10$. Though unrealistic, using $\alpha = 10$ in 1 spatial dimension shows 4 clear, distinct growth phases: 1. within-seed-household exponential growth, 2. constant-speed travelling wave, 3. distribution of infectives gets broader as enough within-household infections overlap in time, and 4. accelerating wave-like solution (though s.d. of spatial distribution also grows exponentially). Comparing with $\alpha = 3, \dots, 6$ and different seeding patterns in 2D (c.f. main Figure 5), we see how these 4 phases overlap to give sub-exponential growth.

Parameter	Min	Max
h	2	8
$v = wp_w$	5	20
p_w	0.1	0.8
R^*	1.3	3

Table S1. Ranges of each parameter value in the Latin hypercube.

Order	Corr.	Grad.
1	0.2599	0.1131
2	-0.7538	-0.4082
3	-0.996	-0.134
4	-0.9972	-0.0163
2 (HH)	-0.9208	-0.2828
4 (HH)	-0.9908	-0.0169

Table S2. Linear correlation coefficients and gradients of linear regression model for main Figures 4B (nodes) and 4C (households).

39 References

- 40 1. Diekmann O (1978) Thresholds and travelling waves for the geographical spread of infection. *J. Math. Biol.* 6(2):109–130.
- 41 2. van den Bosch F, Metz JAJ, Diekmann O (1990) The velocity of spatial population expansion. *Journal of Mathematical*
- 42 *Biology* 28(5):529–565.
- 43 3. Mollison D (1991) Dependence of epidemic and population velocities on basic parameters. *Mathematical Biosciences*
- 44 107(2):255 – 287.
- 45 4. Shaw MW (1995) Simulation of population expansion and spatial pattern when individual dispersal distributions do
- 46 not decline exponentially with distance. *Proceedings of the Royal Society of London. Series B: Biological Sciences*
- 47 259(1356):243–248.